Efficient Techniques for Inductance Extraction of Complex 3-D Geometries

M. Kamon, Massachusetts Inst. of Technology, Cambridge, MA 02139

M. J. Tsuk, Digital Equipment Corporation, Tewksbury, MA 01876

C. Smithhisler, Massachusetts Inst. of Technology, Cambridge, MA 02139

J. White, Massachusetts Inst. of Technology, Cambridge, MA 02139

Abstract

In this paper we describe combining a mesh analysis equation formulation technique with a preconditioned GMRES matrix solution algorithm to accelerate the determination of inductances of complex three-dimensional structures. Results from FASTHENRY, our 3-D inductance extraction program, demonstrate that the method is more than an order of magnitude faster than the standard solution techniques for large problems.

1 Introduction

In high performance VLSI integrated circuits and integrated circuit packaging, there are many cases where accurate estimates of the coupling inductances of complicated three dimensional structures are important for determining final circuit speeds or functionality, the most obvious example being the pin-connect structures used in advanced packaging. For the past decade, volume-element techniques have been used to compute self and coupling inductances of complex three dimensional geometries, but the techniques were intended for geometries which could be represented with at most a few hundred volume filaments. However, the complex structures currently used in integrated circuit packaging can require up to ten thousand filaments to be accurately analyzed. Existing programs become extraordinarily computationally expensive for such large problems, and new algorithms whose computational cost grows more slowly with problem size must be developed.

In this paper we describe how an old equation formulation technique, mesh analysis, can be combined with preconditioned GMRES, a relatively new iterative matrix solution technique, to make FASTHENRY, a fast 3-D inductance extraction program for general packaging structures. We start in the next section by describing a standard approach to the frequency dependent inductance and resistance calculation, in Section 3 we describe the mesh formulation approach, and in Section 4 we briefly describe GMRES. Results from FASTHENRY are given in Section 5, followed by conclusions and acknowledgments.

2 Inductance calculation

One approach to computing the frequency dependent inductance and resistance matrix, denoted Z_r, associated with the terminal behavior of a collection of conductors involves first approximating each conductor as a set of piecewise straight conducting sections. The volume of each straight section is then discretized into a collection of parallel thin filaments through which current is assumed to flow uniformly. The interconnection of these current filaments can be represented with a planar graph, where the n nodes in the graph are associated with connection points between conductor segments, and the b branches in the graph represent the current filaments into which each conductor segment is discretized.

To derive a system of equations from which the resistance and inductance matrix can be deduced, we start by assuming the applied currents and voltages are sinusoidal, and that the system is in sinusoidal steady-state. Following the partial inductance approach in [1, 2], the branch current phasors can be related to branch voltage phasors (hereafter, phasors will be assumed and not restated) by

$$ZI_b = V_b, \qquad (1)$$

0-8186-3010-8/92 $03.00 © 1992 IEEE

where V_b, $I_b \in C^b$, b is the number of branches (number of current filaments), and $Z \in C^{b \times b}$ is the complex impedance matrix given by

$$Z = R + j\omega L, \qquad (2)$$

where ω is excitation frequency. The entries of the diagonal matrix $R \in \Re^{b \times b}$ represent the dc resistance of each current filament, and $L \in \Re^{b \times b}$ is the dense matrix of partial inductances [3]. Specifically,

$$L_{i,j} = \frac{\mu_0}{4\pi} \int_{filament_i} \int_{filament_j} \frac{l_i(X_i) \cdot l_j(X_j)}{|X_i - X_j|} d^3x_i d^3x_j, \qquad (3)$$

where $X_i, X_j \in \Re^3$ are the positions in filament i and j respectively, and l_i, l_j are the unit vectors in the direction of current flow in filaments i and j.

The statement that the branch currents must satisfy Kirchoff's current law, that is, the currents entering each node must sum to zero, can be written using the branch incidence matrix as

$$AI_b = I_s, \qquad (4)$$

where $I_s \in C^n$ is the mostly zero vector of source currents, n is the number of nodes (points where conductor sections meet or a conductor terminates) excluding any reference or ground nodes, and $A \in \Re^{b \times n}$ is the branch incidence matrix.

The node voltages can be related to the branch voltages by

$$A^t V_n = V_b, \qquad (5)$$

where A^t is the transpose of the branch incidence matrix, and $V_n \in C^n$ is the vector of n referenced node voltages. Combining (5) with (4) and (1) yields

$$AZ^{-1}A^t V_n = I_s. \qquad (6)$$

The complex impedance matrix which describes the terminal behavior of the conductor system, Z_r, can by derived from (6) by noting that

$$Z_r \tilde{I}_s = \tilde{V}_s, \qquad (7)$$

where $\tilde{I}_s$ and $\tilde{V}_s$ are the vectors of source currents and voltages. Therefore, the i^{th} column of Z_r can be computed by solving (6) with an I_s whose only nonzero entry corresponds to $\tilde{I}_{s_i}$, and then extracting the elements of V_n corresponding to $\tilde{V}_s$.

In most programs, the dense matrix problem in (6) is solved with some form of Gaussian elimination, and this implies that the calculation grows as b^3, where again b is the number of current filaments into which the system of conductors is discretized [5]. For complicated packaging structures, b can exceed ten thousand, and solving (6) with Gaussian elimination can take days, even using a high performance scientific workstation.

3 Mesh current approach

The approach to calculating the frequency dependent inductance and resistance matrix described above has some disadvantages if (6) is to be solved with an iterative method. It is difficult to apply the iterative method, because the matrix $AZ^{-1}A^t$ contains Z^{-1}, which can only be computed by forming the dense matrix Z, and then somehow inverting it. Another approach to generating a system of equations for the currents and voltages in the network representing the conductor system discretization is mesh analysis [4], and the mesh approach has some advantages which will be made clear below.

To begin, mesh analysis is easiest to describe if it is assumed that the sources attached to the conductor system's terminals generate explicit branches in the graph representing the discretized problem. Kirchoff's voltage law, which implies that the sum of branch voltages around each mesh in the network (a mesh is any loop of branches in the graph which does not enclose any other branches) is represented by

$$MV_b = V_s \qquad (8)$$

where V_b is the vector of voltages across each branch except for the source branches, V_s is the mostly zero vector of source branch voltages, and $M \in \Re^{b \times m}$ is the mesh matrix, where $m = b - s + c$, s is the number of conductor sections and c is the number of conductors. The M matrix has the property that all of its nonzero entries are +1 or -1 and that most of its rows ($m - c$ of them) have no more than two nonzero entries.

The relationship between branch currents and branch voltages given in (1) still holds, and the mesh currents, that is, the currents around each mesh loop, satisfy

$$M^t I_m = I_b, \qquad (9)$$

where $I_m \in C^m$ is the vector of mesh currents. Note that one of the entries in the mesh current vector will be identically equal to the source branch current. Combining (9) with (8) and (1) yields

$$MZM^t I_m = V_s. \qquad (10)$$

The matrix MZM^t is *easily* constructed directly. To compute the i^{th} column of the reduced admittance matrix, $Y = Z_r^{-1}$, solve (10) with a V_s whose only nonzero entry corresponds to $\tilde{V}_{s_i}$, and then extract the entries of I_m associated with the source branches.

Algorithm 1 (GMRES Algorithm for $Ax = b$)

```
guess x⃗⁰
for k = 0,1,... until converged {
  Compute the error, r⃗ᵏ = b⃗ − Ax⃗ᵏ
  Find x⃗ᵏ⁺¹ to minimize r⃗ᵏ⁺¹
    based on x⃗ⁱ and r⃗ⁱ, i = 0,...,k
}
```

4 Using an iterative solver

The standard approach to solving the complex linear system in (10) is Gaussian elimination, but the cost is m^3 operations. For this reason, inductance extraction of packages requiring more than a few thousand filaments is considered computationally intractable. To improve the situation, consider using a conjugate-residual style iterative method like GMRES [7]. Such methods have the general form given in Algorithm 1.

Note that the GMRES algorithm can be directly applied to solving (10), because the matrix MZM^t is easily constructed explicitly. This is not the case for (6). Just to form (6), the Z matrix must first be inverted. This suggests that either some kind of nested GMRES algorithm would be required to solve (6) iteratively, or the matrix would have to be expanded into the sparse tableau, and the GMRES algorithm applied to solving that expanded matrix.

5 Accelerating iteration convergence

In general, the GMRES iterative method applied to solving (10) can be significantly accelerated by *preconditioning* if there is an easily computed good approximation to the inverse of MZM^t. We denote the approximation to $(MZM^t)^{-1}$ by P, in which case preconditioning the GMRES algorithm is equivalent to using GMRES to solve

$$P(MZM^t)I_m = PV_s \qquad (11)$$

for the unknown vector I_m. Clearly, if P is precisely $(MZM^t)^{-1}$, then (11) is trivial to solve, but then P will be very expensive to compute.

A good approximation to $(MZM^t)^{-1}$ that is easily computed can be derived by exploiting the fact that a mesh current in a given conductor is tightly coupled to the other mesh currents within that conductor. With an appropriate numbering of the mesh currents, the interactions between meshes of the same conductor can be clustered into blocks along the diagonal of MZM^t. The inverse of the block diagonal matrix so generated is then an approximation to $(MZM^t)^{-1}$.

Preconditioning with this simple preconditioner proved extremely effective. Table 1 shows the average number of iterations with $tol = 10^{-3}$ for a single solve of the pin package example described in the next section. The number of iterations required by GMRES without the preconditioner increased rapidly with problem size, but with the preconditioner, the iterations remained constant. This result easily makes up for the small cost of calculating the preconditioner.

Size of MZM^t (m)	Iterations WITH precond.	Iterations WITHOUT precond.
210	8	20
560	8	38
910	8	60
1435	8	123
1960	8	164

Table 1: Comparison of the average number of iterations per conductor with and without the preconditioner.

6 Results

In this section we present our results from FASTHENRY. To test the mesh formulation approach, we began with two parallel rectangular wires and compared the results to those in [8]. As a more interesting example, FASTHENRY was used to analyze 35 pins of a 68-pin package from Digital Equipment Corporation. To demonstrate the effectiveness of preconditioned GMRES, times are compared against direct inversion for finer and finer spatial discretization.

For the rectangular wire problem, we considered two parallel copper wires with a 2 mm by 2 mm cross section and 4 mm separation between their centers. The problem is treated as a one conductor problem, with one wire acting as the return path. The data in [8] is for a two dimensional analysis with wires of infinite length, so for this problem the lengths were chosen to be 100 meters and the results scaled appropriately.

To observe how the results varied due to skin and proximity effects, the conductor was divided into various numbers of parallel thin filaments. To follow the

Filaments per conductor section	Size of MZM^t (m)	Solution time, direct inversion	Solution time, preconditioned GMRES
1	35	0.0003	0.007
2	210	0.339	0.147
4	560	8.02	1.08
6	910	35.9	3.08
9	1435	135	7.85
12	1960	344	14.4

Table 2: Execution time comparison for the pin package example. Execution times are in IBM RS6000/540 CPU minutes.

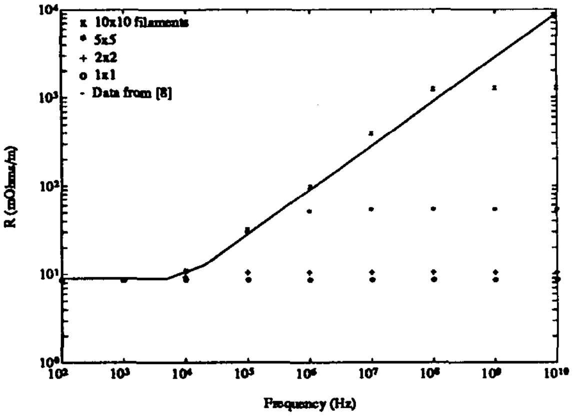

Figure 1: Resistance of Two Long Rectangular Wires

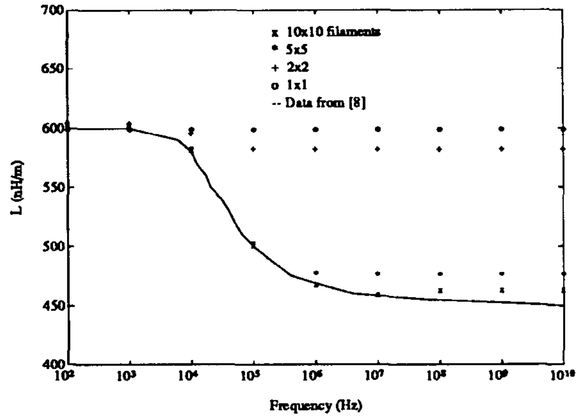

Figure 2: Inductance of Two Long Rectangular Wires

decaying nature of the skin effect, the dimensions of the filaments were chosen to decrease geometrically toward the outer edge of the conductor. FASTHENRY was run with 1, 4, 25, and 100 filaments per wire with the results compared in Figures 1 and 2 against those from [8]. For each case, as the skin depth became much smaller than the smallest filament, the calculated resistance and inductance stopped changing with frequency, as expected. For relatively few filaments per section (e.g. 25) one can determine much of the nature of the impedance. Both the resistance and inductance are accurately determined up to around 10^5 Hz. The resistance results accurately determine the knee of the resistance curve, which shows the beginning of the skin effect. Since it is well known that the resistance increases as the square root of the frequency after the knee, higher frequency resistance values could easily be extracted.

Thirty-five pins of a 68-pin package from DEC, shown in Figure 3, proved a good test of the utility of FASTHENRY. Each pin consists of five conductor sections. Neglecting skin effects and choosing one filament (or branch) per section gives a system of 175 filaments and 35 meshes. Notice that for mesh analysis, the solution is obtained by solving only a 35x35 system, while for the branch incidence matrix approach as in (6) inversion of a 175x175 system is necessary.

To accurately model skin and proximity effects, each conductor section is divided into multiple filaments. As the discretization is refined, the size of the problem grows quickly. For these problems, the advantage of the GMRES algorithm becomes apparent (see Table 2). For twelve filaments per section, GMRES is already 23 times faster than direct inversion. In fact, the number of operations required by GMRES grows only as m^2, while the direct method grows as m^3.

Notice that twelve sections per filament is barely enough to observe skin effects, however memory requirements limit any finer discretizations. It is worth noting that future work to implement multipole algorithms [9] will further reduce both the computational costs and memory requirements, thus allowing finer discretizations.

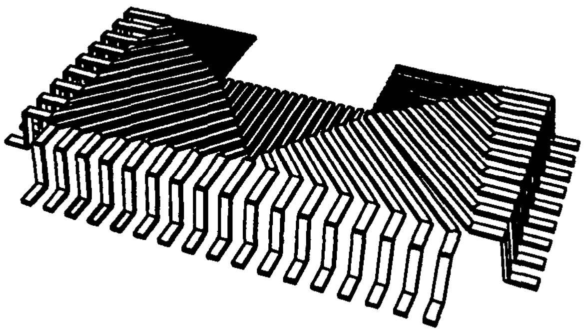

Figure 3: Half of a pin-connect structure. Thirty-five pins shown.

In this paper, we do not give a comparison to the branch incidence approach in (6) since it would require inverting Z, the branch impedance matrix. Z is always larger than MZM^t and would thus be more expensive than direct inversion of MZM^t which is shown in Table 2.

7 Conclusions and acknowledgments

It is shown in this paper that if mesh rather than nodal analysis is used to form the system of equations which must be solved to determine inductance, then the equations can be solved easily with the iterative GMRES algorithm. Addition of the preconditioner to GMRES can reduce the cost of solution to m^2 operations compared to m^3 for direct inversion. Results from FASTHENRY, our 3-D inductance extraction program, demonstrate that the iterative approach can accelerate solution times by more than an order of magnitude.

Future work using multipole algorithms will exploit the fact that the off-diagonal elements of Z are the partial inductances generated from integrals of $\frac{1}{r}$. Such methods will avoid forming and storing most of the entries in the dense matrix MZM^t, and reduce the cost of calculating matrix-vector products required for the GMRES procedure to order b operations.

Currently, FASTHENRY is being extended to include ground planes. Results will be presented at the conference.

The authors would like to thank Keith Nabors, Songmin Kim, Dr. Sami Ali, and Joel Phillips for their help in understanding inductance. In addition, the authors would like to thank Dr. Albert Ruehli, Prof. Raj Mittra, and Dr. Colin Gordon for their helpful suggestions.

This work was supported by the Defense Advanced Research Projects Agency contract N00014-91-J1698, the National Science Foundation contract (MIP-8858764 A02), a National Science Foundation fellowship, and grants from Digital Equipment Corporation and I.B.M.

References

[1] W. T. Weeks, L. L. Wu, M. F. McAllister, and A. Singh, "Resistive and inductive skin effect in rectangular conductors," *IBM Journal of Res. and Develop.*, vol. 23, pp. 652–660, November 1979.

[2] A. E. Ruehli, "Survey of computer-aided electrical analysis of integrated circuit interconnections," *IBM Journal of Research and Development*, vol. 23, pp. 626–639, November 1979.

[3] P. A. Brennan, N. Raver, and A. Ruehli, "Three dimensional inductance computations with partial element equivalent circuits," *IBM Journal of Res. and Develop.*, vol. 23, pp. 661–668, November 1979.

[4] C. A. Desoer and E. S. Kuh, *Basic Circuit Theory.* New York: McGraw-Hill, 1969.

[5] A. E. Ruehli and P. A. Brennan, "Efficient capacitance calculations for three-dimensional multiconductor systems," *IEEE Transactions on Microwave Theory and Techniques*, vol. 21, pp. 76–82, February 1973.

[6] S. M. Rao, T. K. Sarkar, and R. F. Harrington, "The electrostatic field of conducting bodies in multiple dielectric media," *IEEE Transactions on Microwave Theory and Techniques*, vol. MTT-32, pp. 1441–1448, November 1984.

[7] Y. Saad and M. H. Schultz, "GMRES: A generalized minimal residual algorithm for solving nonsymmetric linear systems," *SIAM Journal on Scientific and Statistical Computing*, vol. 7, pp. 856–869, July 1986.

[8] M. J. Tsuk, "Propagation and Interference in Lossy Microelectronic Integrated Circuits," PhD Thesis, Massachusetts Institute of Technology, June 1990.

[9] L. Greengard and V. Rokhlin, "A fast algorithm for particle simulations," *Journal of Computational Physics*, vol. 73, pp. 325-348, December 1987.